Thermodynamics of Aqueous CO_2 Nanobubble Dispersion for Geologic Carbon Storage and Enhanced Oil Recovery

Introduction

Aqueous nanobubble (NB) dispersions have been studied and applied in various industries, such as agriculture and wastewater treatment, which are inherently open systems near atmospheric pressure (Temesgen et al. 2017). The literature is much scarcer for aqueous NB dispersions under high pressures relevant to subsurface applications, such as enhanced oil recovery (EOR) and geologic carbon sequestration; however, recent fundamental studies of aqueous NB dispersions have shown marked differences between near-atmospheric and high-pressure aqueous NB dispersions. For example, the thermodynamic analysis in Achour et al. (2024) explained that a high-pressure aqueous NB dispersion sample contains the gaseous species in two modes: (1) a cluster of bubbles and (2) molecular dispersion in the external aqueous phase that is supersaturated with the gaseous species, and that capillary pressure owing to the presence of small bubbles enables supersaturation. They also demonstrated that the contribution from the second mode can be greater than the first mode to enhance the concentration of the gaseous species above the inherent solubility; therefore, aqueous nanobubble dispersions are referred to as "aqueous NB fluids" to include both modes of CO_2 containment in this paper. Also, experimental data on high-pressure NB fluids [up to 20.8 MPa in Wang et al. (2023) and up to 27.7 MPa in Lawal et al. (2024)] showed that the concentration of gaseous species (CO_2 and N_2) above the inherent solubility increased as the aqueous-phase pressure increased. As Achour et al. (2023) originally pointed out, aqueous NB fluids would find promising subsurface applications if the fundamental understanding of their properties were utilized for practical use cases. Although Wang et al. (2023) reported that the CO_2 concentration in the aqueous NB fluid increases with pressure, the thermodynamic factors that control this concentration at a given injection pressure remain unknown. This paper addresses this question by conducting a thermodynamic analysis of high-pressure aqueous NB fluid based on various types of experimental data.

Theory of Minimum Supersaturation Pressure

Wang et al. (2023) reported the first experimental data for high-pressure aqueous CO_2-NB fluids using deionized water (DI water) at pressures up to 208 bara at 21°C. They found that the CO_2 concentration in their NB samples increased significantly with pressure. The highest CO_2 concentration was 2.3 mol/L, 43% higher than the CO_2 inherent solubility at 208 bara. At 35 bara, however, the CO_2 concentration in the CO_2-NB fluid was near the inherent solubility, highlighting the importance of pressure for supersaturating water with CO_2-NB.

Lawal et al. (2024) reported the first high-pressure core flooding experiments with aqueous CO_2-NB fluids, in which dead oil was displaced in Berea sandstone by three injection fluids, 5-wt% (50,000 ppm) NaCl brine, carbonated NaCl brine, and CO_2-NB in NaCl brine. The inherent solubility of CO_2 in the NaCl brine was 2.09 mol% at 21°C and 158 bara (Duan and Sun 2003). The CO_2-NB had a density of 1.056 g/cm^3 and a viscosity of 1.15 cP at 21°C and 158 bara. The overall composition of the CO_2-NB sample was 3.43 mol% CO_2 and 96.57 mol% NaCl brine. This composition corresponded to a CO_2 concentration of 1.85 mol/L, which is 64% greater than the inherent solubility of CO_2. High-pressure dynamic light scattering measurements showed a multimodal size distribution, with 63% of bubbles having peak diameters at 88.2 nm, 13% at 2.75 μm, and 24% at 6.01 μm. The overall number density of nanoscale and larger bubbles was calculated to be 1.35×10^9 bubbles/cm^3 using a thermodynamic model adapted from Achour et al. (2024) and Achour and Okuno (2020). A supersaturated level of CO_2 concentration in injection water can play an important role in oil displacement (Fuentes-Ibarra et al. 2026).

However, a highly-supersaturated aqueous phase with CO_2 requires the presence of small bubbles with capillary pressure. Achour et al. (2024) presented a spontaneity analysis of aqueous NB fluid and predicted that there exists a critical gas concentration below which nanobubbles are not generated spontaneously. This section presents Achour et al.'s prediction for a critical gas concentration using a more practical set of thermodynamic parameters relevant to EOR. Namely, the fundamental theory of

the minimum supersaturation pressure (MSP) is presented. Spontaneous NB generation is less energetically demanding above the MSP than below it, enabling the aqueous phase to supersaturate. MSP is crucial for the practical deployment of CO_2-supersaturated water for EOR and geologic carbon sequestration. Specific examples in the analysis use the CO_2-NB fluid data presented in Wang et al. (2023); however, the foundational theory presented here is generally applicable to other aqueous NB fluids relevant to subsurface applications.

The thermodynamic description of aqueous NB fluid requires specification of $(N_C + 3)$ variables, where N_C is the number of components (Achour and Okuno 2020). The analysis in this paper specifies the components' mole numbers, the external aqueous-phase pressure, temperature, and bubble diameter using a thermodynamic model adopted from Achour et al. (2024) and Achour and Okuno (2020). The term "supersaturation" generally refers to the overall CO_2 concentration in the aqueous NB fluid above the inherent CO_2 solubility in the aqueous fluid at the temperature and pressure; for example, in the data of Wang et al. (2023), the supersaturation was 43% relative to the inherent solubility at 21°C and 208 bara. Achour et al. (2024) described that the supersaturation mechanism in aqueous NB fluid is closely related to the aqueous-phase composition, which lies in the metastable region of the Gibbs or Helmholtz free energy in the presence of a cluster of nanobubbles.

Using the thermodynamic model applied to aqueous NB samples with CO_2 and DI water in Wang et al. (2023), the CO_2 concentration in the aqueous phase was analyzed for two systems, (1) carbonated DI water with no capillary pressure or a CO_2-phase diameter of infinity, and (2) aqueous CO_2-NB fluid with bubbles of uniform diameter 100 nm, at 21°C for varying pressures. Both correspond to CO_2 solubility in CO_2-saturated water, but with different bubble sizes: ∞ and 100 nm, denoted $x_{S\infty}$ and x_{S100nm}. Figure 1 shows that the deviation of x_{S100nm} from $x_{S\infty}$ diminishes as the external aqueous-phase pressure increases, levels off between 49.0 and 49.5 bara, and eventually becomes insensitive to pressure at higher pressures. The MSP can be practically defined as the breakpoint in this plot for the specified components, bubble size, and temperature; however, the MSP for the aqueous CO_2-NB fluid has a rigorous thermodynamic mechanism as presented later.

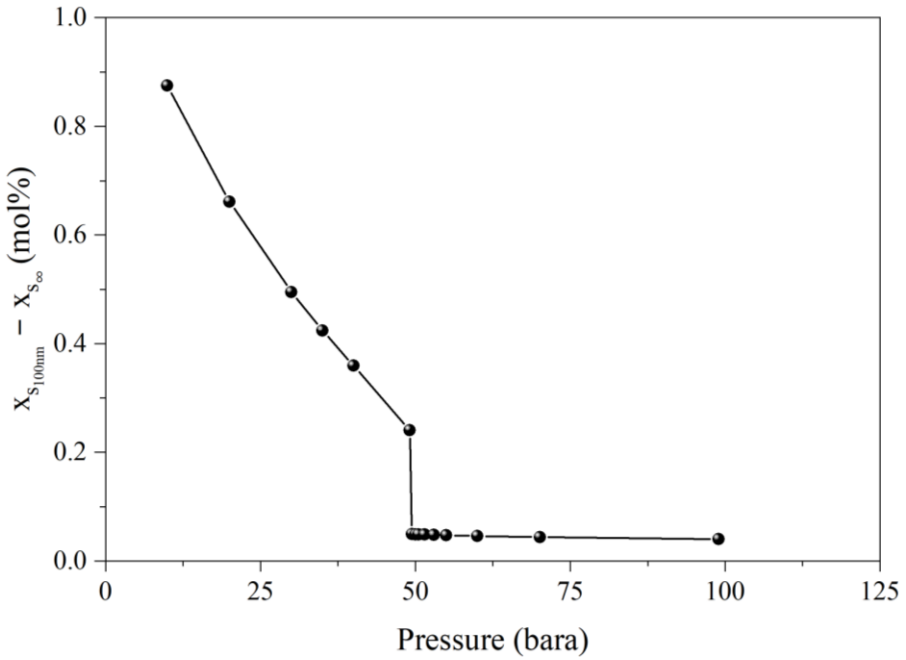

Figure 1 *The deviation of CO_2 solubility in water with bubble diameter 100 nm (x_{S100nm}) from that with a planar interface (no capillary pressure; $x_{S\infty}$) at 21°C based on a thermodynamic model (Achour et al. 2024) calibrated using the data in Wang et al. (2023). The minimum supersaturation pressure (MSP) can be practically defined as the breakpoint in this plot for the specified components, bubble size, and temperature (i.e., 49.5 bara in this figure); however, the MSP for the aqueous CO_2-NB fluid has a rigorous thermodynamic mechanism as presented in this paper.*

The Gibbs free energy analysis explains why MSP occurs. Figure 2a shows the Gibbs free energy surfaces for the aqueous CO_2-NB sample at 10 bara and 21°C, in the presence of bubbles with a diameter of 100 nm. The red line represents the tangent in the absence of NB (i.e., no capillary pressure or infinite bubble diameter), while the green line represents the tangent for the NB system, connecting the Gibbs free energy surface of the aqueous phase to that of the NB phase. The different slope between the two tangent lines causes a marked difference between $x_{S\infty}$ and x_{S100nm}; that is, the NB formation would require the CO_2 concentration in the aqueous phase to be more than double the CO_2 concentration in the absence of NB, which was referred to as a critical gas concentration in Achour et al. (2024).

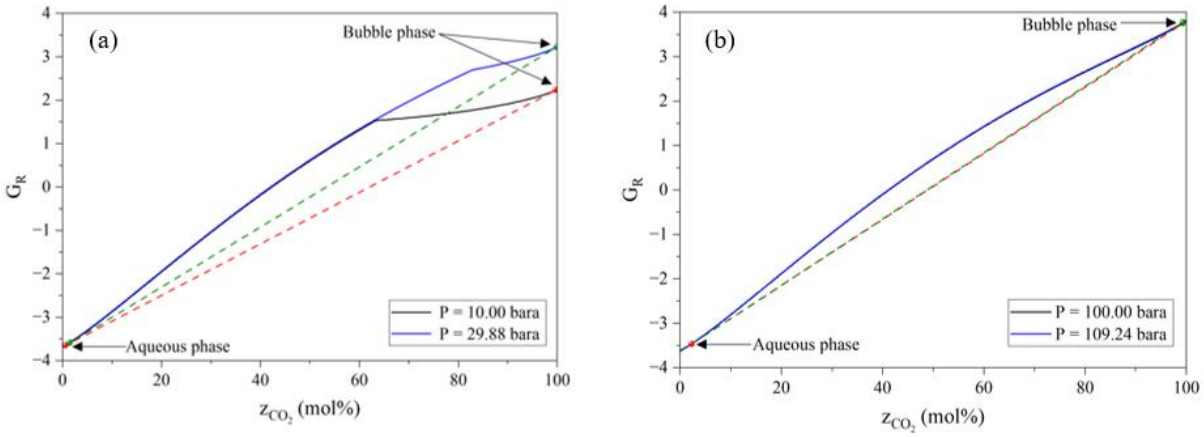

Figure 2 *Reduced molar Gibbs free energy for water-CO_2 mixtures: (a) 21°C and 10 bara; (b) 21°C and 100 bara. The red line shows the tangent line connecting the equilibrium vapor and liquid phase compositions at 100 bar. The green line shows the tangent line connecting the equilibrium vapor and liquid phase compositions in the presence of capillary pressure.*

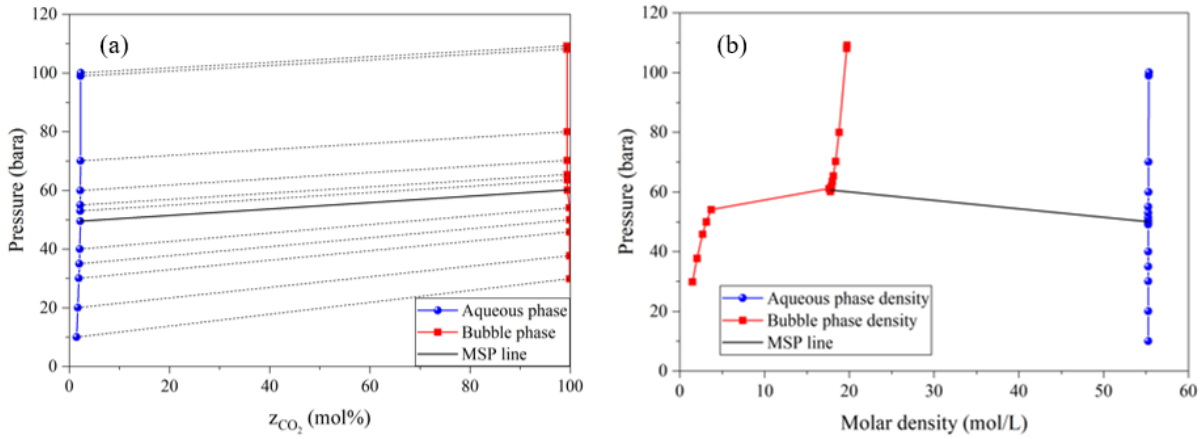

Figure 3 *Phase properties for the aqueous CO_2-NB at 21°C with bubble diameter 100 nm using a thermodynamic model (Achour et al. 2024) calibrated based on the data from Wang et al. (2023): (a) pressure-composition diagram; (b) pressure-density diagram. In (a), the dashed lines represent the tie-lines connecting the aqueous and the NB phase. The MSP tie-line is represented by the solid black line. The NB-phase composition changes at the MSP tie-line. In (b), the solid black line connects the NB and aqueous phases at MSP. The MSP for the aqueous CO_2-NB fluid corresponds to the pressure at which the NB phase transitions from a vapor-like to a liquid-like state*

By contrast, the Gibbs free energy analysis for an external pressure of 100 bara (Figure 2b) shows that $x_{S\infty}$ and x_{S100nm} are nearly identical, indicating that the CO_2 concentration in the aqueous phase is insensitive to bubble size. This finding is crucial for the practical deployment of aqueous NB fluid for subsurface applications because the insensitivity identified in this research suppresses interphase mass transfer of CO_2, even with a bubble-size distribution and any perturbation in thermodynamic conditions,

and because it fundamentally explains why the CO_2 concentration is much more enhanced by aqueous NB fluid at higher pressures, as experimentally demonstrated by Wang et al. (2023).

Interestingly, the marked difference in $|x_{S100nm} - x_{S\infty}|$ between the two pressures, 10 bara and 100 bara, in Figure 2 stems from the properties of the other phase, the CO_2-rich bubble phase. Figure 3a presents a pressure-composition (P-x) diagram for the NB system over a range of pressures. The blue and red lines represent the mole fraction of CO_2 in the aqueous and NB phases, respectively. The dashed lines represent tie-lines connecting the aqueous-phase composition to the NB-phase composition. The tie-lines are not horizontal because of capillary pressure. The MSP tie-line (solid black line) marks a transition in the NB-phase composition and density. The CO_2 concentration in the NB phase decreases slightly relative to that below the MSP. The pressure-density plot (Figure 3b) shows that the NB phase transitions from a vapor-like to a liquid-like CO_2-rich phase with increasing pressure. Therefore, the MSP for the aqueous CO_2-NB fluid corresponds to the pressure at which the NB phase transitions from a vapor-like to a liquid-like state; hence, the CO_2 vapor pressure (and its extension) is useful in estimating the CO_2-NB MSP.

Conclusions

There is a pressure above which spontaneous NB generation is less energetically demanding than below it. This pressure is called the minimum supersaturation pressure (MSP). It is desirable to generate aqueous NB fluid above the MSP to achieve effective gas supersaturation of the aqueous phase for subsurface injection. For aqueous CO_2-NB fluid specifically, the MSP is the pressure at which the density of the CO_2-rich bubble phase approaches a liquid-like value as the external aqueous-phase pressure increases.

Acknowledgements

We gratefully acknowledge the sponsors of the Energi Simulation Industrial Affiliate Program on Sustainable Energy Expansion “Energi X” at the University of Texas at Austin (UT Austin). Ryosuke Okuno holds the H. B. (Burt) Harkins, Jr. Professorship in Petroleum Engineering at UT Austin.

References

Achour, S.H. and Okuno, R. 2020. Phase Stability Analysis for Tight Porous Media by Minimization of the Helmholtz Free Energy. *Fluid Phase Equilibria,* **520**: 112648. https://doi.org/10.1016/j.fluid.2020.112648

Achour, S.H., Sheng, K., Lawal, T., and Okuno, R. 2023. Thermodynamic Modeling of Aqueous Nanobubble Dispersion. Paper presented at the SPE Annual Technical Conference and Exhibition, San Antonio, Texas, USA. https://doi.org/10.2118/215122-MS

Achour, S.H., Lawal, T., Sheng, K., and Okuno, R. 2024. Thermodynamic Modeling of Aqueous Nanobubble Dispersion. *SPE Journal,* **29**(06): 3204-3222. https://doi.org/10.2118/215122-PA

Duan, Z. and Sun, R., 2003. An Improved Model Calculating CO_2 Solubility in Pure Water and Aqueous NaCl Solutions from 273 to 533 K and from 0 to 2000 bar. Chemical geology, 193(3-4): 257-271. https://doi.org/10.1016/S0009-2541(02)00263-2

Fuentes-Ibarra, D., Oyenowo, O.P., and Okuno, R., Analysis of Oil Displacement by Aqueous Nanobubble Dispersion of CO_2, SPE Improved Oil Recovery Conference, April 21 – 23, 2026, Tulsa, Oklahoma. https://doi.org/10.2118/231595-MS

Lawal, T., Wang, H., and Okuno, R. 2024. Aqueous Nitrogen-Nanobubble Dispersion and Supersaturation at Elevated Pressures up to 277 bara. *Journal of Molecular Liquids,* **398**, 124340. https://doi.org/10.1016/j.molliq.2024.124340

Temesgen, T., Bui, T.T., Han, M., et al. 2017. Micro and Nanobubble Technologies as a New Horizon for Water-Treatment Techniques: A Review. Advances in Colloid and Interface Science 246(August): 40–51. https://doi.org/10.1016/j.cis.2017.06.011

Wang, H., Lawal, T., Achour, S.H., Sheng, K., and Okuno, R. 2023. Aqueous Nanobubble Dispersion of CO_2 at Pressures up to 208 bara. *Energy & Fuels,* **37**(24): 19726-19737. https://doi.org/10.1021/acs.energyfuels.3c03660